Al-Mustansiriyah Journal of Science
ISSN: 1814-635X (print), ISSN:2521-3520 (online) Volume 34, Issue 3, 2023 DOI: http://doi.org/10.23851/mjs.v34i3.1373

Research Article **Open Access**

Quantitative Analysis of Blurry Color Image Fusion Techniques using Color Transform

Nawras Badeaa Mohammed[1], Haidar Mohamad[1*], Heba Kh. Abbas[2], Ali Aqeel Salim[3]

[1]Department of Physics, College of Science, Mustansiriyah University, 10052 Baghdad, Iraq.
[2]Department of Physics, College of Science for Women, Baghdad University, 10071 Baghdad, Iraq.
[3]Laser Center and Physics Department, Faculty of Science, Universiti Teknologi Malaysia, 81310 Johor Bahru, Johor, Malaysia

*Correspondent contact: haidar.mohamad@uomustansiriyah.edu.iq

Article Info

Received
17/04/2023

Revised
21/05/2023

Accepted
28/05/2023

Published
30/09/2023

ABSTRACT

This work focuses on fused color images resulting from motion blur (left and right) with a blur block size of 11 pixels. The color conversion process was performed from RGB color space (Red, Green, Blue) to HSV (Hue, Saturation, Value), L*a*b*, and Ycbcr (Luminance, Chrominance) color space. The traditional (addition, multiplication) and proposed fusion techniques (absolute real standard deviation) were used for this purpose. The data was examined by quality criteria with reference (Mutual Information, Correlation Coefficient, Structural Content, Normalized Cross Correlation) and without reference (Blind Reference less Image Spatial Quality Evaluator, Naturalness Image Quality Evaluator, and Perception-based Image Quality Evaluator). In results and depending on the criteria, the best fusion method is the proposed real standard deviation.

KEYWORDS: Motion Blur, Color Space Transformation, Fusion Techniques, Quality Criteria.

الخلاصة

أنتج هذا العمل صورًا مدمجة ناتجة عن ضبابية الحركة (يسارًا ويمينًا) بحجم كتلة ضبابية يبلغ ١١ بكسل. كان هذا بعد إجراء عملية تحويل اللون من مساحة ألوان RGB إلى مساحة ألوان HSV و L * a * b * و Ycbcr. يتم استخدام تقنيات الاندماج التقليدية (الجمع والضرب) وتقنيات الاندماج المقترحة (الانحراف المعياري الحقيقي المطلق) لهذا الغرض. البيانات التي تم فحصها بواسطة معايير الجودة مع الصورة الأصلية (المعلومات المتبادلة، معامل الارتباط، المحتوى الهيكلي، الارتباط المعياري عبر الارتباط) وبدون مرجع (المرجع أقل مقيّم جودة الصورة المكانية، مقيم جودة الصورة الطبيعية، ومقيّم جودة الصورة القائم على الإدراك). في النتائج وبالاعتماد على المعايير، كانت أفضل طريقة دمج هي طريقة الانحراف المعياري الحقيقي المقترح.

INTRODUCTION

Image fusion is the process of merging information between two or more images to obtain a fused image with integral information, high quality, and other advantages; it can be performed using different methods, such as pixel-level fusion, feature-level fusion, and decision-level fusion, depending on the specific application and requirements [1]. It saves time and reduces costs by acquiring multiple images of the same scene or object. This can be particularly useful in applications such as medical imaging, where multiple scans can be expensive and time-consuming, object recognition, target tracking, image segmentation, remote sensing, and military reconnaissance, including remote sensing, air, environmental and military surveillance, robotics, and other fields [2].

In 2021, Ayodeji Salau *et al*. [3] assessed the results of a fused image (white flower) using discrete wavelet transform (DWT) and discrete cosine transform (DCT) techniques. The red, green, blue (RGB), and intensity hue saturation (IHS) values for single and merged images were evaluated. The signal-to-noise ratio (SNR) showed different results for DWT and DCT for similar values. Wang *et al*. (2022) [4], presented

bilinear interpolation and perceptual color spaces (HSL, HSV, LAB, and LUV) fusion techniques to improve multispectral spatial and spectral characteristics for different satellite data (Orbview-3and Landsat-7) for the same region images. The SNR fidelity criterion for achromatic information was calculated in addition to the mean color shifting parameters, which calculate the ratio of chromatic information loss of the RGB compound within each pixel to assess the quality of the fused images. The combined image quality results were not affected by using the LAP color space, unlike the LUV color space, which recorded the worst results. Zhaoyang Hou *et al.* (2023) [5] proposed a parameter-adaptive dual-channel pulse-coupled neural network in the domain of non-subsampled shearlet transform based on the low-frequency sub-band fusion process; the visual feature fusion rule was low-level. They used entropy, mutual information, Gradient averaging, spatial frequency, spectral distortion, and visual information resolution; the proposed method has the best fusion effect.

This study seeks to enhance the visual quality of distorted images using the image fusion method. This will be achieved by applying horizontal (left and right) motion blur techniques to the input images. It then converts the distorted images from RGB to HSV, LAB, and Ycbcr. The fused image techniques included addition, multiplication, standard, and deviation. The quality of the fused images was tested with different criteria.

MATERIALS AND METHODS

In order to improve the clarity of distorted images, researchers have proposed image fusion techniques that include distorting the input images using the motion blur method horizontally left and right [6], followed by traditional mathematical techniques such as addition and multiplication [7], or statistical fusion techniques based on weights (standard deviation) [8]. The general form of the motion blur function [9] is given as follows:

$$h(i,j) = \begin{cases} \frac{1}{L} \; if \sqrt{i^2+j^2} \le \frac{L}{2} and \; \frac{i}{j} = -tan(\phi) \\ 0 \qquad\qquad otherwise \end{cases} \qquad (1)$$

Motion length (L) and direction (ϕ) are the two essential parameters.

Color Transform Method

Using a mathematical method, the color transformation technique transforms the image from a color space like RGB to a different space [10]. It is one of the essential techniques in information integration analyses that integrate multispectral information to improve color and characteristics and enhance information. These methods were used to assess the quality and the improvement of information generated by the integration process using HSV[11], L*a*b* [12], and Ycbcr methods [13].

A set of standard quality criteria were used within this work to evaluate the spectral and spatial similarities between merged image (C) and input images (A and B). Two quality analysis criteria were used, one with a reference image and one without a reference image [14]. When a reference image is available [15], the performance of the merged image is assessed using Mutual Information (MI) [16], Correlation Coefficient (CC) [17], Structural Content (SC), and Normalized Cross Correlation (NCC) [14]. However, if the reference image is not available, the performance of the merged image is assessed using metrics such as *Structural Blind/Reference less Image Spatial Quality Evaluator (BRISQUE)* [18], Naturalness Image Quality Evaluator (NIQE) [19], Perception-based Image Quality Evaluator (PIQE) [15].

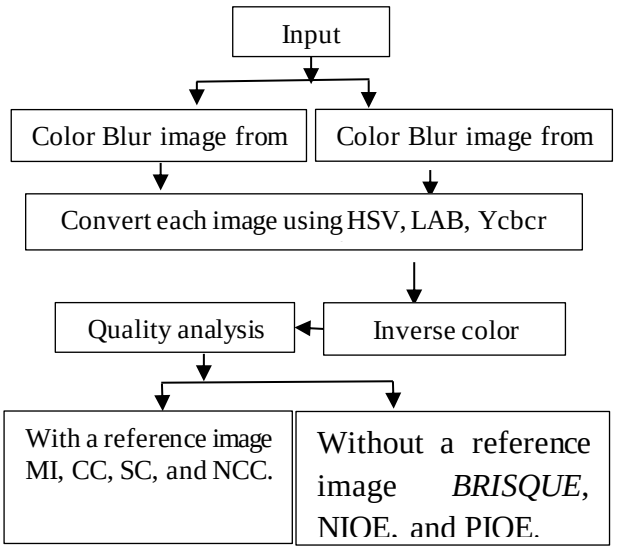

Figure 1: The flowchart of the proposed algorithm for obtaining the fused image.

ISSN: 1814-635X (print), ISSN:2521-3520 (online) Volume 34, Issue 3, 2023 DOI: http://doi.org/10.23851/mjs.v34i3.1373

The Proposed Algorithms

Fuse Images Based on the Conversion from (RGB) To (HSV) Algorithm

Fusion algorithms based on color conversion (HSV) involve converting the image from the RGB color space to the HSV color space. Subsequently, the images are fused using approved merging methods, which include addition, multiplication, and standard deviation.

Start Algorithm

Step 1: load color blur image (I Right) and (I Left) based image data store function
Step 2: transform color map image to HSV color map image
Step 3: Separation of the third compounds for the first image I1=Y1(:,:,3)and second image I2=Y2(:,:,3).
Step 4: Apply Fuse Equation C-add =I1/2+I2/2;
Step 5: Apply Fuse Equation C-multi =sqrt(double(I1)).*sqrt(double(I2));
Step 6: Apply Fuse Equation C-std (i, j)=p1* I Right (i,j)+(1-p1)* I Left (i,j) where the corresponding pixels is multiplied by various factors as the following: Proposed method P1= Standard deviation I Right/ (Standard deviation I Right+ Standard deviation I Left)
Step 7: return of the third compounds for the first image Y1(:,:,3)=C(add, multi, and std)
Step 8: transform HSV colormap to an RGB colormap.
Step 9: Save images using *im* write function

End

Fuse images based on the conversion from (RGB) to (LAB) algorithm

Fusion algorithms based on color conversion (LAB) include converting the image from space (RGB) to space (LAB), and then the images were merged using the approved fusion methods, the method of addition, multiplication, and standard deviation.

Start algorithm

Step 1: load color blur image I Right and I Left based image data store function
Step 2: transform color map image to LAB color map image
Step 3: Separation of the first compounds for the first image I1=Y1(:,:,1)and second image I2=Y2(:,:,1).
Step 4: Apply Fuse Equation C-add =I1/2+I2/2;
Step 5: Apply Fuse Equation C-multi =sqrt(double(I1)). *Sqrt(double(I2));
Step 6: Apply Fuse Equation C-std (i, j) =p1* I Right (i,j)+(1-p1)* I Left (i ,j) where the corresponding pixels is multiplied by various factors as the following: Proposed method P1= Standard deviation I Right/ (Standard deviation I Right+ Standard deviation I Left)
Step 7: return of the first compounds for the first image Y1(:1) =C (add, multi, and std)
Step 8: transform LAB color map to an RGB color map.
Step 9: Save images using *imwrite* function

End

Fuse images based on the conversion from (RGB) to (Ycbcr) algorithm.

Fusion algorithms based on color conversion (Ycbcr) include converting the image from space (RGB) to space (Ycbcr), and then the images were fused using the approved fusion methods, the method of addition, multiplication, and standard deviation.

Start algorithm

Step 1: load color blur image I Right and I Left based image data store function
Step 2: transform color map image to Ycbcr color map image
Step 3: Separation of the first compounds for the first image I1=Y1(:,:,1)and second image I2=Y2(:,:,1).
Step 4: Apply Fuse Equation C-add =I1/2+I2/2;
Step 5: Apply Fuse Equation C-multi =sqrt(double(I1)).*sqrt(double(I2));
Step 6: Apply Fuse Equation C-std (i, j)=p1* I Right (i,j)+(1-p1)* I Left (i,j) where the corresponding pixels is multiplied by various factors as the following: Proposed method P1= Standard deviation I Right/ (Standard deviation I Right+ Standard deviation I Left)
Step 7: return of the first compounds for the first image Y1(:,:,1)=C(add, multi, and std)
Step 8: transform Ycbcr color map to an RGB color map.
Step 9: Save images using imwrite function

End

RESULTS AND DISCUSSION

In the study, images shown in Figure 2 were relied upon, which include Figure 2(a) Lina with a size of (512×512), Figure 2 (b) personal with a size of (931×1280), and Figure 2 (c) pepper with a size of (640×480). All images have 24-bit depth per pixel.

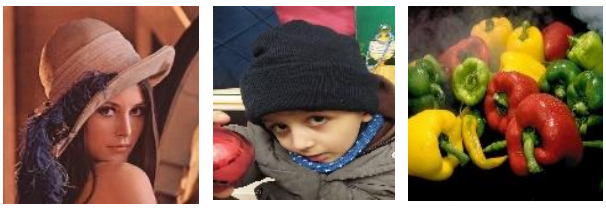

(a) (b) (c)

Figure 2: The images approved in the study (a) Lena, (b) personal, and (c) pepper.

The motion blur method was applied to the images in Figure 2 with block sizes of 11 pixels. The block was shifted from left to right once and from right to left, as shown in Figure 3.

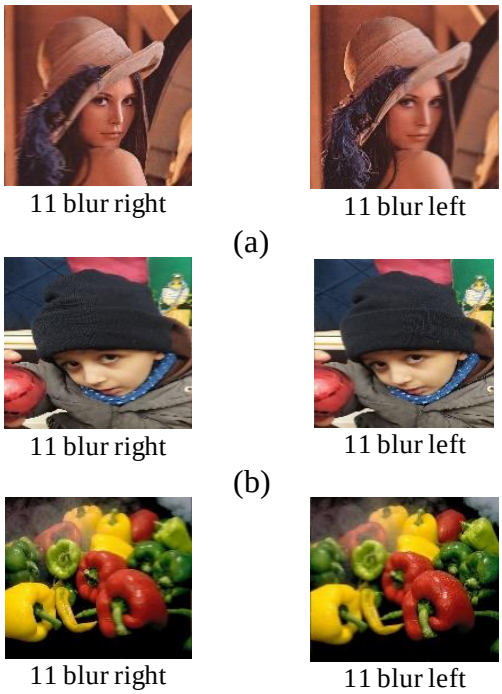

Figure 3: The images resulting from the process of motion blur towards the left and right for (a) Lena, (b) personal (c) pepper.

The color transformation was achieved using color transformation HSV, LAB, and Ycbcr. The methods of Addition, Multiplication, and Standard deviation (std) were used as fusion methods, as shown in Figures (4-6).

Figure 4: Lena Fusion image after color transformation with (a) HSV, (b) LAB, and (c) Ycbcr

Figure 5: Personal Fusion image after color transformation with (a) HSV, (b) LAB, and (c) Ycbcr

Al-Mustansiriyah Journal of Science
ISSN: 1814-635X (print), ISSN:2521-3520 (online) Volume 34, Issue 3, 2023 DOI: http://doi.org/10.23851/mjs.v34i3.1373

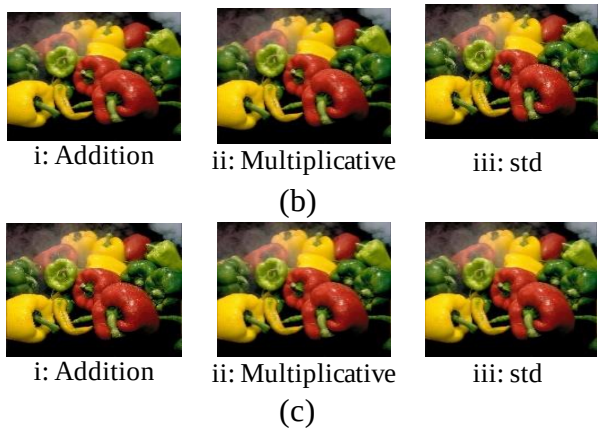

Figure 6: Pepper Fusion image after color transformation with (a) HSV, (b) LAB, and (c) Ycbcr.

Figure 7 shows the statistical criteria data with reference for the blur right image (A), blur left image (B), and fused image (C). Figure 7(i) is the Mutual Information criteria data. Figure 7(i) (a, c, e) between A and C. While Figure 7(i) (b, d, f) between B and C. The three images' data in Figure 7(i) are divided as Lena in (a, b), pepper (c, d), and personal in (e, f). This sequence order is the same for the remaining parts in Figure 7. Figure 7(ii) Normalized cross-correlation criteria. Figure 7(iii) is the correlation criteria. Finally, Figure 7(iv) structural content criteria.

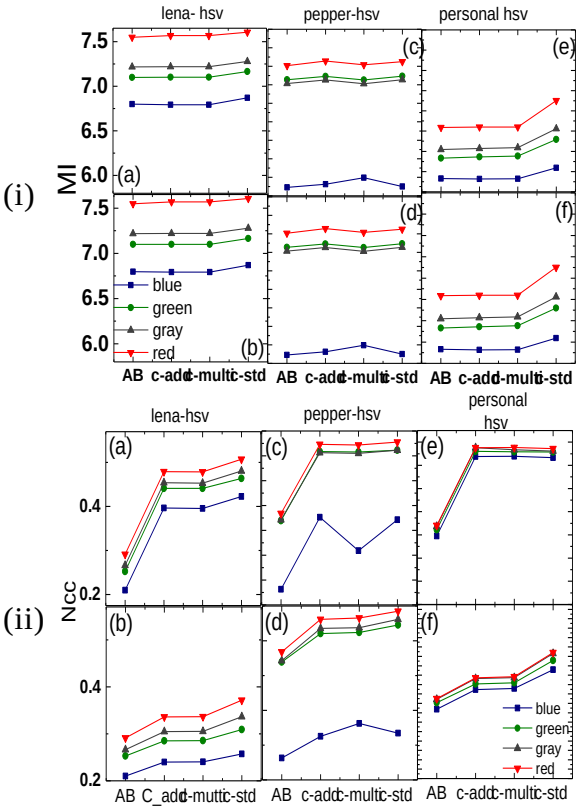

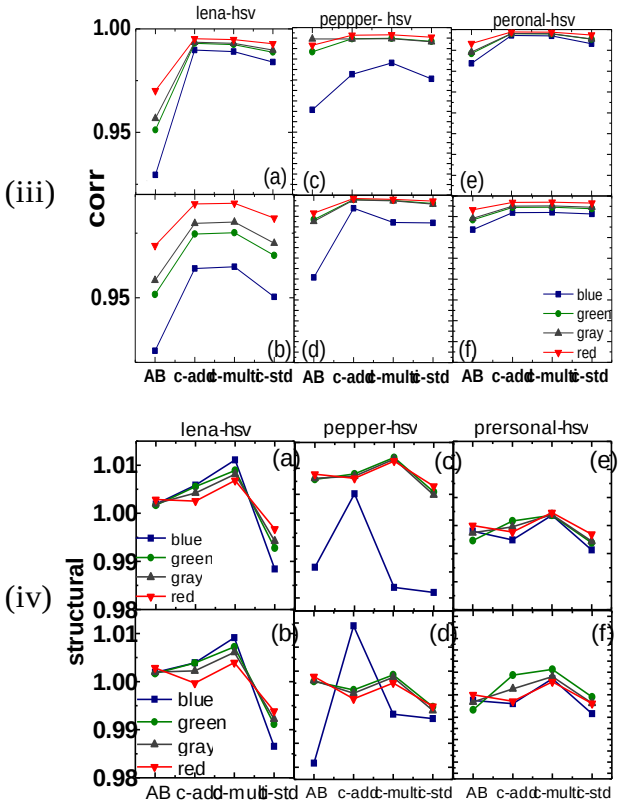

Figure 7: Image quality evaluation with reference-based criteria for images before and after fusion techniques using HSV transform.

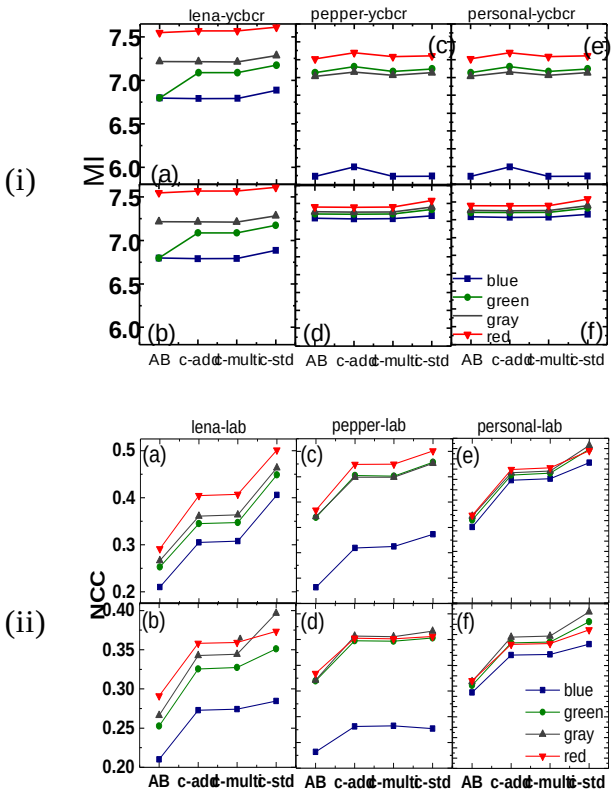

(iii)

(iv)

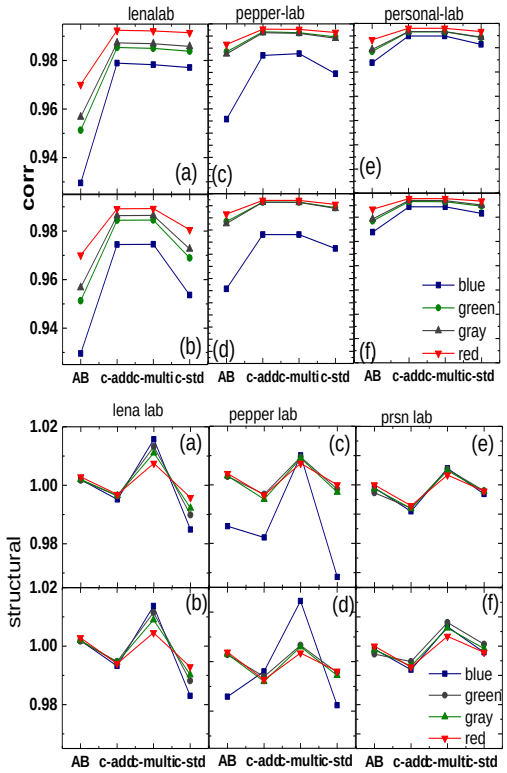

Figure 8: Evaluation of image quality with reference-based criteria for images before and after the fusion techniques using LAB transform

Figure 8 shows the Mutual Information criteria used for the statistical criteria concerning the blur right image (A), blur left image (B), and fused image (C). Figure 8(i) (a, c, e) between A and C. While figure 8(i) (b, d, f) between B and C. The three images' data in Figure 8(i) are divided as Lena in (a, b), pepper (c, d), and personal in (e, f). This sequence order is the same for the remaining parts in Figure 8. Figure 8(ii) is the Normalized cross-correlation criteria data. Figure 8(iii) is the correlation criteria data. Finally, Figure 8v is structural content criteria data.

(i)

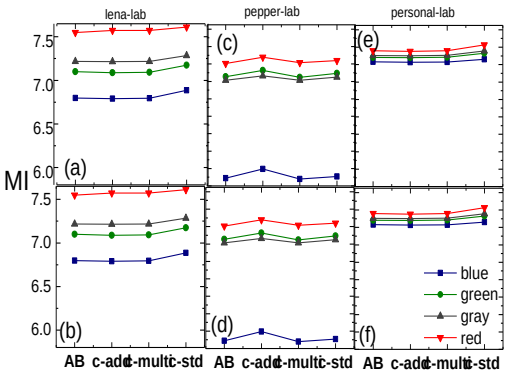

(ii)

(iii)

(iv)

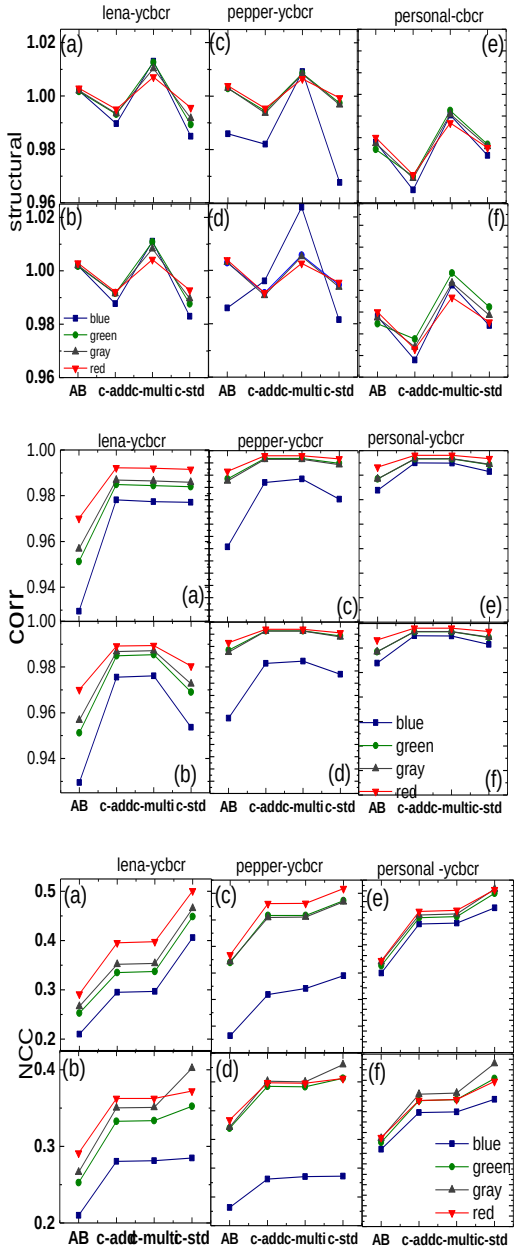

Figure 9: Evaluation of image quality with reference-based criteria for images before and after the fusion techniques using Ycbcr transformation.

Figure 10 shows the statistical criteria without reference for the blur right image (A), blur left image (B), and fused image (C). The three images' data in this figure are divided as Lena in (a), pepper (b), and personal in (c). Figure 10(i) is the Structural Blind/Reference less image spatial quality evaluator. Figure 10(ii) naturalness image quality evaluator criteria. Finally, Figure 10(iii) perception-based image quality evaluator.

Al-Mustansiriyah Journal of Science
ISSN: 1814-635X (print), ISSN:2521-3520 (online) Volume 34, Issue 3, 2023 DOI: http://doi.org/10.23851/mjs.v34i3.1373

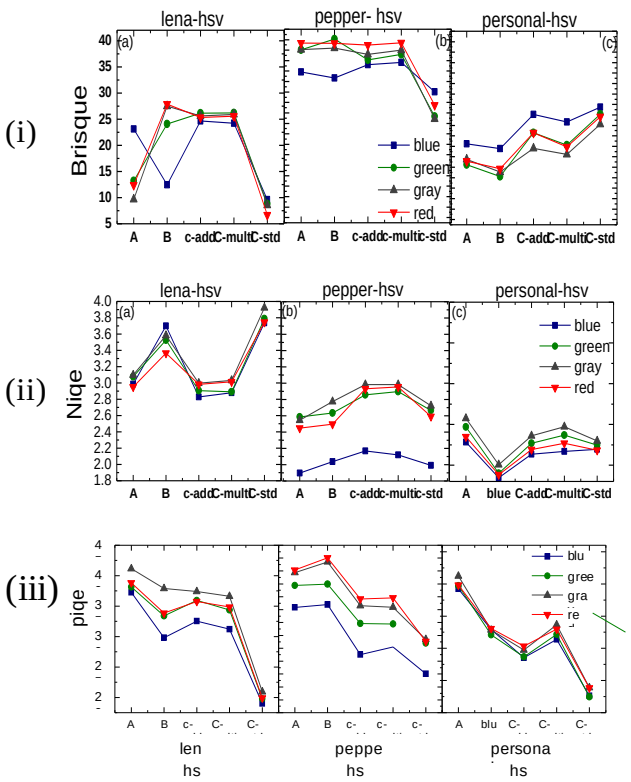

Figure-10 Evaluation of image quality without reference-based criteria for images before and after the fusion techniques using HSV transform.

Figure 11 shows the statistical criteria without reference. The three images data in Figure 11 are divided as Lena in (a), pepper (b), and personal in (c). Figure 11(i) is the Structural Blind/Reference less Image Spatial Quality Evaluator. Figure 11(ii) Naturalness Image Quality Evaluator criteria. Finally, Figure 11(iii) perception-based image quality evaluator.

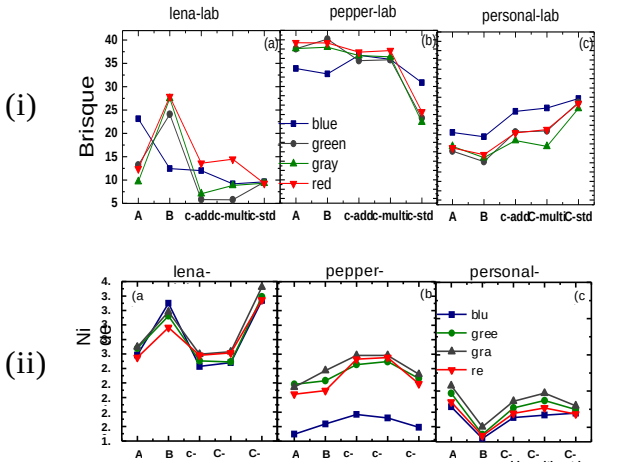

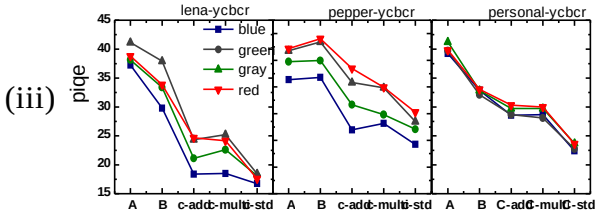

Figure 11: Evaluation of image quality without reference-based criteria for images before and after the fusion techniques using LAB transform.

Figure 12 shows the statistical criteria without reference for the blur right image (A), blur left image (B), and fused image (C). The three images' data in Figure 12 are divided as Lena in (a), pepper (b), and personal in (c). Figure 12(i) is the Structural Blind/Reference less Image Spatial Quality Evaluator.

Figure 12(ii) naturalness image quality evaluator criteria. Finally, Figure 12(iii) perception-based image quality evaluator.

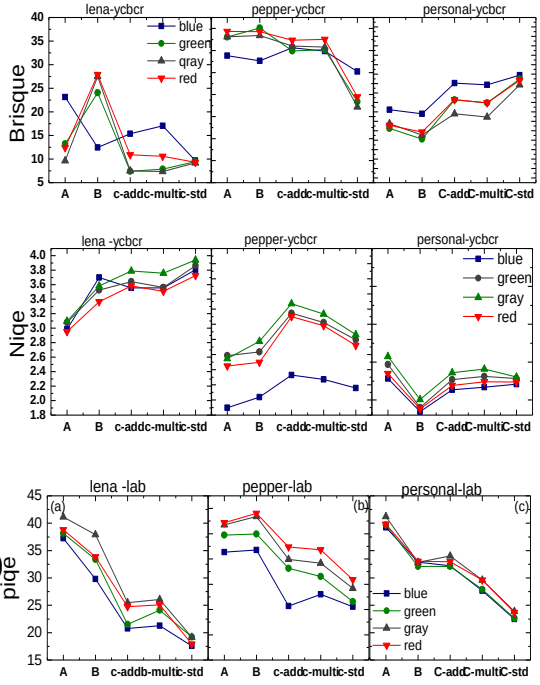

Figure -12 Evaluation of image quality without reference-based criteria for images before and after the fusion techniques using Ycbcr transform.

Discussion

In Figure 7, the normalized cross-correlation criteria have increasing behavior with the fusion techniques, where the standard deviation technique increased highly, as well as the cross-

correlation criteria. It was noticed that its behavior increased with the fusion techniques, especially in Lena's image, while the behavior of the structural standard decreased with merging techniques and deviation techniques. Figure 8 shows that the Mutual Information criterion has fluctuating and constant behavior with fusion techniques. In contrast, the cross-correlation criterion has different behavior in the image of Lena. In contrast, the pepper and personality images behave similarly to the Normalized cross-correlation criterion. The increase was apparent with fusion techniques, particularly in the standard deviation technique. An apparent decrease in the Structural content criterion was observed, especially in the standard deviation technique, where the decrease in the standard is evidence of quality efficiency.

From Figure 9, the behavior of the Mutual Information standard was constant with fusion techniques. Regarding Normalizes, cross-correlation increased with fusion techniques, especially the standard deviation technique, while cross-correlation contrasted in the Lena image. The image of Pepper and the personal image was similar in behavior. The decrease was apparent with fusion techniques in the Structural content criteria, indicating the criterion's efficiency in the evaluation process. In Figures (10, 11, and 12), the Brisque results contrasted with the fusion techniques, and an apparent decrease in the standard deviation technique and the Niqe standard gave almost similar results to the Brisque standard regarding the Piqe criterion. The results were clear, and the values increased, especially with the standard deviation technique.

CONCLUSIONS

The blurred image was simulated using the linear homogeneous motion blur technique with a block size of 11 pixels. The linear direction is from right to left. Color transformations (HSV, Lab, and YCbCr) were applied to the blurred images. Fusion methods (addition, multiplicative, and real standard deviation) were used with three color images. The performance of these methods was evaluated using ten types of criteria, with six using reference and four without reference. The best combination method was found to be real standard deviation.

Disclosure and Conflicts of Interest: The authors advertise that they have no conflicts of interest.

REFERENCES

[1] Abbas, H.K., et al., New algorithms to enhanced fused images from auto-focus images. Baghdad Sci. J, 2021. 10(18): p. 1.

[2] Abbas, H.K., et al., Adopting Image Integration Techniques to Simulate Satellite Images. Iraqi Journal of Science, 2020: p. 3445-3455.

[3] Salau, A.O., S. Jain, and J. NnennaEneh, A review of various image fusion types and transform. Indonesian Journal of Electrical Engineering and Computer Science, 2021. 24(3): p. 1515-1522.

[4] Wang, X., et al., A unified multiscale learning framework for hyperspectral image classification. IEEE Transactions on Geoscience and Remote Sensing, 2022. 60: p. 1-19.

[5] Hou, Z., et al., A Remote Sensing Image Fusion Method Combining Low-Level Visual Features and Parameter-Adaptive Dual-Channel Pulse-Coupled Neural Network. Remote Sensing, 2023. 15(2): p. 344.

[6] Zhou, W., et al., Improved estimation of motion blur parameters for restoration from a single image. Plos one, 2020. 15(9): p. e0238259.

[7] Li, S., et al., Pixel-level image fusion: A survey of the state of the art. Information Fusion, 2017. 33: p. 100-112.

[8] Al-Mokhtar, Z.T., F.N. Ibraheem, and H.F. Al-Layla, A Review of Digital Image Fusion and its Application. Al-Rafidain Engineering Journal (AREJ), 2021. 26(2): p. 309-322.

[9] Askari Javaran, T. and H. Hassanpour, Using a Blur Metric to Estimate Linear Motion Blur Parameters. Computational and Mathematical Methods in Medicine, 2021. 2021: p. 1-8.

[10] Al-Jasim, A.A.N., T.A. Naji, and A.H. Shaban, The Effect of Using the Different Satellite Spatial Resolution on the Fusion Technique. Iraqi Journal of Science, 2022: p. 4131-4141.

[11] Perez-Udell, R.A., A.T. Udell, and S.M. Chang, An automated pipeline for supervised classification of petal color from citizen science photographs. Applications in Plant Sciences, 2023: p. e11505.

[12] Yee, A.L.K., et al., Preliminary analysis of rock mass weathering grade using image analysis of CIELAB color space with the validation of Schmidt hammer: A case study. Physics and Chemistry of the Earth, Parts A/B/C, 2023. 129: p. 103291.

[13] Dwivedi, R. and V.K. Srivastava. An Imperceptible and Robust image watermarking using RDWT and SVD in YCbCr color space. in 2022 IEEE 9th Uttar Pradesh Section International Conference on

Electrical, Electronics and Computer Engineering (UPCON). 2022. IEEE.
[14] Wu, L. and L. Zhao. ISAR Image Registration Based on Normalized Correlation Coefficient. in 2023 IEEE 3rd International Conference on Power, Electronics and Computer Applications (ICPECA). 2023. IEEE.
[15] Golestaneh, S.A., S. Dadsetan, and K.M. Kitani. No-reference image quality assessment via transformers, relative ranking, and self-consistency. in Proceedings of the IEEE/CVF Winter Conference on Applications of Computer Vision. 2022.
[16] Zhou, M., et al. Mutual information-driven pan-sharpening. in Proceedings of the IEEE/CVF Conference on Computer Vision and Pattern Recognition. 2022.
[17] Lu, W., et al. Blind Surveillance Image Quality Assessment via Deep Neural Network Combined with the Visual Saliency. in Artificial Intelligence: Second CAAI International Conference, CICAI 2022, Beijing, China, August 27–28, 2022, Revised Selected Papers, Part II. 2023. Springer.
[18] Gwon, G.-H., et al., CNN-based Image Quality Classification Considering Quality Degradation in Bridge Inspection using an Unmanned Aerial Vehicle. IEEE Access, 2023.
[19] Wu, L., et al., VP-NIQE: An opinion-unaware visual perception natural image quality evaluator. Neurocomputing, 2021. 463: p. 17-28.

How to Cite

N. B. . Mohammed, H. Mohamad, H. K. Abbas, and A. A. . Salim, "Quantitative Analysis of Blurry Color Image Fusion Techniques using Color Transform", *Al-Mustansiriyah Journal of Science*, vol. 34, no. 3, pp. 132–140, Sep. 2023.